Renewable and Sustainable Energy Reviews 97 (2018) 377–389

Contents lists available at ScienceDirect

Renewable and Sustainable Energy Reviews

journal homepage: www.elsevier.com/locate/rser

Proposed method for contracting of wind-photovoltaic projects connected to the Brazilian electric system using multiobjective programming

Giancarlo Aquila[a], Luiz Célio Souza Rocha[b], Edson de Oliveira Pamplona[a], Anderson Rodrigo de Queiroz[c], Paulo Rotela Junior[d,*], Pedro Paulo Balestrassi[a], Marcelo Nunes Fonseca[e]

[a] Institute of Production Engineering and Management, Federal University of Itajuba, Itajuba, MG, Brazil
[b] Federal Institute of Education, Science and Technology, North of Minas Gerais, Almenara, MG, Brazil
[c] School of Business, Decision Sciences Department, North Carolina Central University, Durham, NC, USA
[d] Department of Production Engineering, Federal University of Paraiba, Joao Pessoa, PB, Brazil
[e] Department of Production Engineering, Federal University of Goias, Aparecida de Goiania, GO, Brazil

ARTICLE INFO

Keywords:
Renewable energy sources
Multiobjective programming
Normal boundary intersection
Brazilian electricity system
Wind-PV farms

ABSTRACT

Owing to the wind and photovoltaic (PV) potential in Brazil, the country has recently seen increased exploration into the construction of wind-PV hybrid plants. However, as specific criteria for contracting this type of project have not yet been developed, this paper presents a model to assist the government in contracting projects that maximize the socioeconomic well-being of the Brazilian electricity sector. For this, multiobjective programming is used to simultaneously handle two objective functions—maximally reducing emission density and minimizing the levelized cost of electricity (LCOE)—with the aid of the mixture arrangement technique. In this respect, the optimization method called normal boundary intersection (NBI) is applied to solve the multiobjective problem and construct the Pareto frontier. Additionally, a metric based on the ratio between entropy and the global percentage error (GPE) is used to identify the optimal Pareto solution. The model was applied to determine optimal configurations for wind-PV powerplants in twelve Brazilian cities, and the results obtained reveal the capacity of the model to indicate the optimum configuration according to the wind and PV potential of each city.

1. Introduction

In recent decades, Brazil has implemented strategies to encourage the use of renewable energy sources (RES) in order to reduce the dependence of large hydroelectric plants on its energy matrix [1]. The rationing and blackouts that occurred in the country between 2001 and 2002 were a significant motivator for the government to mobilize and promote the use of new energy sources—especially RES [2]. Since then, the country has introduced sources such as wind, biomass, small hydroelectric power stations, and more recently, photovoltaic (PV) in incentive programs and incentive contract environments [3].

In 2014, low hydroelectric reservoir levels led to a jump in energy prices in the market which further reinforced discourse on the need to promote alternatives to hydroelectric dams in Brazil [4]. At the end of the same year, for the first time, PV energy participated in an auction, and in April 2015 an Alternative Source Auction—LFA—contracted three wind farms. Additionally, in 2015, there were the New Energy Auctions with the participation of wind energy, and the Reserve Energy Auctions with the participation of solar and wind energy [5]. These events signal the country's intention to intensify the use of these sources, which are capable of diversifying the energy matrix and increasing sustainability in the electric system.

Due to the wind and solar potential in the country, the use of hybrid generation from wind-PV plants is timely, and becoming a reality with the recent construction of several wind-PV power projects [6]. Trannin [7] points out that advantages of power generation from these hybrid systems include: complementarity of sources, since the wind regime is more intense at night, while the incidence of sun occurs during the day; economies of scale, reducing the average cost to companies that invest in both sources; and that only one environmental impact study is necessary for a project that uses both sources, which accelerates the environmental licensing process.

However, the two sources also have specific disadvantages. In the case of wind power, according to Fadigas [8], among some of the main

* Correspondence to: Cidade Universitaria s/n, Joao Pessoa, PB 58051-900, Brazil.
E-mail addresses: giancarlo.aquila@yahoo.com (G. Aquila), luiz.rocha@ifnmg.edu.br (L.C. Souza Rocha), pamplona@unifei.edu.br (E. de Oliveira Pamplona), arqueiroz@ncsu.edu (A.R. de Queiroz), paulo.rotela@gmail.com (P. Rotela Junior), pedro@unifei.edu.br (P.P. Balestrassi), marcelo_nunes@ufg.br (M.N. Fonseca).

https://doi.org/10.1016/j.rser.2018.08.054
Received 8 May 2018; Received in revised form 23 August 2018; Accepted 28 August 2018
Available online 07 September 2018
1364-0321/

disadvantages are: the visual pollution caused in the places where wind powerplants are installed; noise pollution due to the sound of the wind blowing on the blades; and the impact of aero generators on birds of the region—potential to cause death to animals that collide with the aero generators. Additionally, based on Ramanathan [9], it is observed that the wind and biomass plants occupy a significant area, and for this reason, the construction of wind powerplants can cause the de-characterization of the natural habitat where they are installed, increase land expenses, and limit the option of future enterprise expansion.

In relation to solar energy, the main disadvantages are: the lack of energy production at night [10]; technology still in the stage of maturation with the levelized cost of electricity (LCOE) still higher than that of other RES, such as wind and biomass [11]; and in places of medium to high latitudes, production falls sharply during the winter.

In this respect, an interesting alternative that combines the advantages of wind power and PV for the production of electricity, while reducing the impact of the disadvantages of each source, is the wind-PV hybrid system. In addition to being more reliable and less expensive [12], optimally sized hybrid generation projects maximize the potential of natural resources, such as sun and wind [13]. In many cases, a degree of complementarity among sources, the possibility of optimization of operating and investment costs, and the reduction of social and environmental impacts are pointed out. Based on these arguments, some generator agents have proposed specific energy auctions for the contracting of wind-PV hybrid plants, thereby seeking to expand the space for new projects, bypassing several constraints of the transmission system for wind energy and PV [6].

Considering that investors are beginning to show interest in wind and PV sources in the form of hybrid projects, it is important to develop mathematical models that guide the government in bidding processes aimed at contracts that use the two sources simultaneously. Thus, the present study aims to develop a method capable of assisting the government in the bidding process so as to contract grid-connected, wind-PV power generation projects that are optimally configured from the economic and socio-environmental perspectives.

To achieve this goal, multiobjective programming is used to guide the contracting of projects that simultaneously reduce CO_2 emissions per occupied area, as well as minimize the LCOE. Thus, LCOE modeling and CO_2 emission reduction were carried out using a mixture arrangement technique and, later, the normal boundary intersection (NBI) methodology was used to perform the multiobjective optimization of the functions in the study. The proposed method will be applied to analyze the best configuration for a hybrid plant in the following twelve Brazilian cities: Araripina, in Pernambuco (PE); Braganca Paulista, in the state of Sao Paulo (SP); Campo Grande, in Mato Grosso do Sul (MS); Jundiai, in the state of Sao Paulo (SP); Laguna, in Santa Catarina (SC); Macau, in Rio Grande do Norte (RN); Mineiros, in Goiás (GO); Montes Claros, in Minas Gerais (MG); Mossoro, in Rio Grande do Norte (RN); Parnaiba, in Piaui (PI); Rio Grande, Rio Grande do Sul (RS); and Xique-Xique, in Bahia (BA).

2. Multiobjective programming

Impacts of power generation projects have become increasingly critical, and project planning has become increasingly complex. Therefore, Oree et al. [14] argue that classic formulations, such as models that include cost minimization as a sole objective, are becoming less realistic, and it is necessary to consider more attributes in the energy planning process.

Models that aim only to minimize costs are free of conflict between two or more objectives and therefore the solution can be found when the function reaches its optimum. In this case, no special method is needed [15]. However, when the optimization problem encompasses more than one objective, the complexity increases because the objectives are functions of the same decision variables and conflict with each other [16]. In order to study the trade-off between conflicting objectives and explore the available options, it is necessary to formulate an optimization problem from methods capable of working with multiple objective functions. The following mathematical expression demonstrates a typical multiobjective optimization problem:

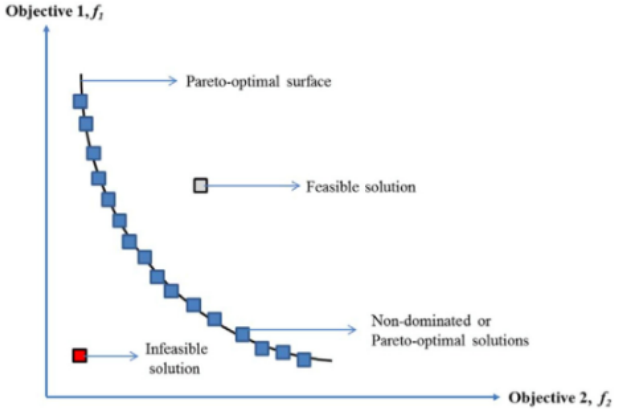

Fig. 1. Pareto frontier for a minimization problem with two objectives. Source: Oree, et al. [14].

$$Min.\ F(x) = \{f_1(x), f_2(x), \ldots f_k(x)\}^T$$
$$s.\ t.\ :\{x \in \mathbb{R}^n | g_r(x) \leq 0,\ r \in I,\ h_q(x) = 0,\ q \in J\} \quad (1)$$

where: $F(x)$ is the vector of objective functions (f_i) consisting of k criteria, which are mutually conflicting; x is the vector of decision variables; g_r and h_q are the functions of restriction of inequality and equality, respectively; I and J are the index sets containing as many elements as inequality and equality constraints, respectively.

The models developed from these methods assist in identifying a satisfactory solution from a set of non-dominated, or Pareto-optimal solutions. In Fig. 1, the efficient frontier (or Pareto frontier) for a problem with two objectives is represented.

According to Shahraki and Noorossana [17], solution strategies for multiobjective problems can be divided into two methods: prioritization and agglutination. The first is the optimization of one goal, subject to constraints that involve the other goals. Among the examples of this solution strategy are: ε-method [15] and lexicographic programming [18]. The second is characterized by converting all objective functions into one, thereby reducing the original problem [19]. Among the main agglutination methods are: goal programming [20]; the global criterion method [15]; the weighted sum method [21]; and the NBI [22].

With regard to solving energy planning problems with optimization models, it is possible to find studies in the literature that similarly seek to propose new solutions. Initially, studies such as Park et al. [23], Kannan et al. [24], and Sirikum et al. [25] used formulations that included only cost minimization as the main objective. However, problems related to energy planning often involve multiple objectives that generally conflict with one another [26–28]. According to Aghaei et al. [29], the most common objectives in energy planning involve cost minimization, environmental impacts, and adequate system reliability.

Recently, the NBI method has been used in several studies to solve energy planning problems. Aghaei et al. [29] developed a multiobjective programming model from the NBI, aiming at power generation expansion planning that prioritizes the following objectives: minimization of costs and environmental impacts, as well as maximization of reliability. Vahidinasab and Jadid [30] formulated a model for the strategy of contracting generation projects for an electric system, taking into account the minimization of power flow (combined with coefficients that represent the emission of pollutants), maximization of individual return for investors, and physical constraints of power generation.

Izadbakhsh et al. [31] developed an optimization model to

determine the best combination of wind turbines, PV panels, fuel oil generators, and battery banks to form a small, isolated generation system. In programming, the NBI method is used with two objective functions—one concerning minimization of the total cost of the system, and the other for the minimization of pollutant emissions.

The NBI is based on a geometric method of intuitive parameterization to produce a set of points at the Pareto frontier—even for non-convex problems—and is considered an efficient technique for the comparison between solutions distributed evenly at the Pareto frontier [22]. The NBI approach uses the following equation to solve multi-objective optimization problems [22]:

$$\begin{aligned} &\underset{(x,D)}{MaxD} \\ &s.t.: \overline{\Phi} w - D\overline{\Phi} e = \overline{F}(\mathbf{x}) \\ &\mathbf{x} \in \Omega \end{aligned} \tag{2}$$

where: w is the convex weighting; D is the distance between the utopia line and the Pareto frontier; $\overline{F}(\mathbf{x})$ is the vector containing the individual values of the normalized objectives; e is a column vector of value 1; Φ and $\overline{\Phi}$ are the payoff matrix and the normalized payoff matrix, respectively, and can be written as:

$$\Phi = \begin{bmatrix} f_1^*(x_1^*) & \cdots & f_1(x_m^*) \\ \vdots & \ddots & \vdots \\ f_m(x_1^*) & \cdots & f_m^*(x_m^*) \end{bmatrix} \Rightarrow \overline{\Phi} = \begin{bmatrix} \frac{f_1^*(x_1^*) - f_1^*(x_1^*)}{f_1(x_m^*) - f_1^*(x_1^*)} & \cdots & \frac{f_1(x_m^*) - f_1^*(x_1^*)}{f_1(x_m^*) - f_1^*(x_1^*)} \\ \vdots & \ddots & \vdots \\ \frac{f_m(x_1^*) - f_m^*(x_m^*)}{f_m(x_1^*) - f_m^*(x_m^*)} & \cdots & \frac{f_m^*(x_m^*) - f_m^*(x_m^*)}{f_m(x_1^*) - f_m^*(x_m^*)} \end{bmatrix} \tag{3}$$

The solution that minimizes the i-th objective function $f_i(x)$ can be represented as $f_i^*(x_i^*)$. When it replaces the optimal individual x_i^* in the remaining objective functions, we have $f_i(x_i^*)$.

As a criterion for choosing the optimal Pareto frontier solution constructed from the NBI, the present study will use a measure that corresponds to the maximum value of the ratio between the entropy and global percentage error (GPE). The measure of entropy allows finding an optimal point with maximum diversification in a system with different components. In systems characterized as mixtures, the percentage of each component of the blend follows a discrete probability distribution, (p). In this sense, based on Shannon [32], the entropy calculation can be described according to Eq. (4):

$$H = -\sum_{i=1}^{m} p_i \log p_i \tag{4}$$

where: p_i = percentage of the variables that are part of the system to be diversified.

The use of entropy is justified because it is a measure that assumes the maximum value when the results in a probability distribution are equally probable and therefore compatible with the objectives of increasing the diversification of the Brazilian energy matrix.

The GPE that is associated with an error measure. Rocha et al. [33] explains that when used to determine the optimal weights of a multi-objective problem, the GPE calculates the sum of the differences of the Pareto-optimal solutions in relation to their targets, which are represented by the utopia line. The GPE calculation is formulated as follows:

$$\text{GPE} = \sum_{i=1}^{m} \left| \frac{y_i^* - T_i}{T_i} \right| \tag{5}$$

where: y_i^* = optimal value of the answers; T_i = target value; m = number of problem objectives.

Therefore, it is a proposed criterion that can value both the questions related to energy planning and those that consider the relation of the solution obtained by the NBI method with the values of utopia. The formulation of the weighting method to be used is indicated by Eq. (6) [34].

$$\xi = \frac{H}{\text{GPE}} \tag{6}$$

where: ξ = measure resulting from the ratio between entropy and GPE.

3. Materials and methods

The proposed method can support the agencies of the Brazilian electricity sector in the bidding process with regard to the contracting of wind-PV power generation projects connected to the network with optimal configurations—taking into account economic and socio-environmental aspects. Since there are no ready-made models that address the problem of optimizing the proportion of each installed power source in a wind-PV project, according to the circumstances in which these projects are inserted in Brazil, we used the design of experiments (DOE) by mixture arrangement to model the objective functions.

Regarding the definition of response variables, the proposed model considers one objective related to socio-environmental issues and another that involves the economic-financial scope. Thus, the objectives are defined as: maximally reducing emission density (tons of CO2/km^2), denominated as y_1; and minimization of LCOE (R$/MWh), defined as y_2.

3.1. Objectives to be optimized

3.1.1. Reduced emission density

Bertoldi et al. [35] state that RES are closely related to environmental preservation and mitigation of climate change. In this respect, wind and PV energy are among RES that do not require fossil fuels [36].

Wind forms from the continuous circulation of layers of air in the atmosphere. In this process, the main factors influencing air circulation—both on a global and local scale—are solar radiation and the Earth's rotation [37]. In the case of PV energy, it is possible to state that the sun is the most abundant energy source available on the planet. The production of electricity from this source occurs through the conversion of solar radiation using PV panels, a parabolic trough, or mirrors. In the production of electricity from PV energy, both the voltage and current are dependent on the radiation that reaches the conversion technology [38]. Thus, we can say that producing energy with wind and PV systems may result in reduced CO_2 emissions [36].

Maximally reduced emission density meets one of ANEEL's goals for the electricity sector, which involves maximizing the benefits of each energy resource, while minimizing negative impacts on the environment and society [39]. The measure is related to socio-environmental issues, since it measures the amount (provided by a clean generation project) of avoided CO_2 emission, per km^2. To find the value, we simply divide the product of an emission factor with the energy production, by the sum of the areas occupied by each source that constitute the project.

From the calculation of the production of wind power and PV, it is possible to estimate the resulting reduction in CO_2 emission. In Eq. (7) the reduced emission calculation is described.

$$ER = F_e E_p \tag{7}$$

where: ER = reduced CO_2 emission in tons of CO_2 (tCO_2); F_e = emission factor (tCO_2/MWh); and E_p = total energy production (MWh).

In Eq. (8), the formula for the calculation of reduced emission density is described. The values of 9.9 for wind power coefficient (Pw) and 0.63 for PV power (Ppv) refer to the area (in km^2) occupied by each installed mega-watt (MW) of wind and solar power and were calculated from data in Table 1. Table 1 lists the areas in km^2 occupied by each installed giga-watt (GW) of each source.

$$\rho_{red} CO_2 = \frac{F_E \sum E_{pm}}{9.9P_w + 0.63P_{pv}} \tag{8}$$

where: $\rho_{red}CO_2$ is the reduced CO_2 emission density, per year (tCO_2/

Table 1
Space occupied by GW installed from each source.
Source: Ramanathan [9].

Source	Occupied land area in km² per GW installed
Biomass	25,600
Wind	**9900**
Hydropower	7600
Solar FV	**630**
Thermoelectric	35
Oil	20
Natural Gas	20
Nuclear	10

km²); and E_{pm} is the monthly average energy production (MWh).

3.1.2. Levelized cost of electricity

LCOE will be estimated from Eq. (9), which is characterized as the most traditional method used to calculate this element [40]. This method relates the total cost of power generation with the plant's physical guarantee (PG). The expenses directly related to power generation are: disbursement with the investment in the project; operation and maintenance costs (O&M); and project interest payments. The PG corresponds to the maximum capacity that can be negotiated in contracts for the purchase and sale of energy in a given period [41].

$$LCOE = \frac{\sum_{t=0}^{T} \frac{C_t}{(1+i)^t}}{\sum_{t=0}^{T} \frac{E_{p_t}}{(1+i)^t}} \quad (9)$$

where: C_t = total power generation costs for a given period, t; T = final period of the analysis horizon; E_{p_t} = PG of the plant in each period, t; i = discount rate.

The weighted average cost of capital (WACC) was used for the discount rate in the LCOE calculation. This methodology is used in several studies that analyze investments in projects generating power from RES—such as those of Rocha et al. [42], Aquila et al. [43], Aquila et al. [1], Ondracek et al. [44] and Ertürk [45]—and is recommended by the Clean Mechanism's Executive Board in the Annex Guidelines on the Assessment of Investment Analysis [46]. Eq. (10) presents the formulation for the WACC calculation.

$$WACC = k_d D(1-\tau) + k_e E \quad (10)$$

where: k_d = the debt cost; D = fraction of debt (%); τ = income tax rate; k_e = cost of equity; E = fraction of equity (%).

For the present study, the WACC was deflated by US inflation, according to ANEEL [47]. Table 2 presents the parameters for the WACC calculation.

For the calculation of k_d, the same methodology as that of Ertürk [45] (and as indicated by ANEEL [47]) for companies investing in the electricity sector was applied. The methodology corresponds to the calculation of a portion resulting from the sum of the risk-free rate, the credit risk premium, and the country risk premium. The calculation is given in Eq. (11).

Table 2
Parameters used to calculate the WACC.

Parameter	Value	Source
D	63.55%	Damodaran [48]
E	36.45%	Damodaran [48]
r_f	5.64%	ANEEL [47]
r_c	3.37%	ANEEL [47]
r_b	2.62%	ANEEL [47]
r_m	13.20%	ANEEL [47]
β	1.14	Damodaran [48]
k_d	11.63%	Eq. (11)
k_e	16.88%	Eq. (12)
US inflation	2.41%	ANEEL [47]
WACC	11.03%	Calculated
WACC (deflated)	8.42%	Calculated

$$k_d = r_f + r_c + r_b \quad (11)$$

where: r_f = risk-free rate; r_c = credit risk premium; r_b = country risk premium.

For the calculation of k_e, the capital asset pricing model (CAPM) was used. The model—originally presented by Sharpe [49], added to the country risk—is widely used in the literature, as in the studies of Aquila et al. [1], and Ertürk [45]; as well as recommended by ANEEL [47]. The calculation is presented in Eq. (12).

$$k_e = r_f + \beta \times (r_m - r_f) + r_b \quad (12)$$

where: r_m = market risk premium; β = beta, which measures the risk of the project in relation to the market.

In Brazil, wind and solar power generation projects are contracted in auctions for a period of 20 years and receive support from the BNDES financing lines. The financing can be requested by companies with headquarters and administration within the country and legal entities governed by public law. The minimum amount to be financed is R$ 20 million and, in the present study, the interest rate used (discounted for inflation) was 4.99%. Until April 2017, the amortization period for wind power projects was 16 years, with that of solar projects at 20 years. For all projects, there is a grace period of six months, with interest, beginning at the start of project operations.

3.2. Mixture arrangement

The mixture arrangement is the only DOE technique capable of providing a means of determining the formulation for a specific blend [50]. With regard to the experimental mixture arrangement, the factors are components or ingredients of a mixture. Therefore, there is a relationship of dependence between the composition levels [51]. Consequently, this establishes a totality constraint for the levels of the components that are part of the blend. In this respect, suppose that $x_1, x_2, \ldots, x_p$ represent the proportions of p components. With this, according to Cornell [50], the constraints are presented as: $x_1 + x_2 + \ldots + x_p = 1$ and $0 \leq x_p \leq 1$.

The experimental scenarios formed in the mixture arrangement are configured from a simple coordinate system. As such, in this context, simplex arrangements are the most commonly used [50]. The planning of a simplex *lattice*, with p components and polynomial model adjusted in order m, is made from $m+1$ proportions, equally spaced between 0 and 1, and tested for each factor in the design [51]. The levels of factors x_i are obtained as follows:

$$x_i = 0, \frac{1}{m}, \frac{2}{m}, \ldots, 1; \text{ for } i = 1, 2, \ldots, p \quad (13)$$

All combinations or mixtures are used; the number of experiments (N) in the simplex *lattice* is given by:

$$N = \frac{(p+m-1)!}{m!(p-1)!} \quad (14)$$

In the case analyzed, the mixture arrangement was configured for a grid-connected, wind-PV project with a total power of 30 MW, which corresponds to the maximum power that allows the entrepreneur a discounted transmission and distribution system usage tariff. After carrying out the reduced emission density and LCOE calculations for each configuration, quadratic regressions were performed to obtain the objective functions for the two *outputs*.

In the present study, to estimate the objective functions representing the reduced emission density and LCOE, experimental scenarios are first generated from the mixture arrangement to guide the calculations of the reduced emission density per year, and the annual LCOE for each are subsequently analyzed. The configuration of the arrangement was based on the simplex *lattice*, with two components (wind power and

Table 3
Scenarios generated by the mixture arrangement.

x_1 Power relative to wind power source (MW)	x_2 Power relative to solar source (MW)
30.0	0.0
24.0	6.0
22.5	7.5
18.0	12.0
15.0	15.0
12.0	18.0
7.5	22.5
6.0	24.0
0.0	30.0

PV), five degrees *lattice*, as well as the central and axial points of the arrangement—totalizing nine experimental scenarios. Table 3 shows the experimental scenario generated from the mixture arrangement for each of the twelve cities.

3.3. 3.3 Calculations for the production of energy by wind and PV sources

With regard to energy trading contracts in Brazil, according to Moreno et al. [52], power generation enterprises must guarantee 100% of the PG. For the construction of the model directed to wind-PV powerplants, the PG estimate is fundamental for the reduced emission density and LCOE calculations. However, as in the present study, it will not be considered for real projects. Instead, the PG measurement will be made from the average annual wind and PV production estimated from different location analyses.

3.3.1. Wind power production

A wind turbine captures part of the kinetic energy of the wind as it passes through the area swept by the rotor and is subsequently transformed into electrical energy. The average annual wind energy production is estimated from the product of wind power (as described by Amarante [53]), the number of operating hours of the plant's wind turbines (equivalent to 8760), and losses due to unavailability and technical issues in the transmission system (equal to 3% and 4%, respectively) [54,55]. In Eq. (15), the calculation of the annual production of the windmill portion of the plant is described.

$$E_{P_{li}} = \frac{8760 \times 0.93}{2} \rho A_r v^3 C_P \eta \quad (15)$$

where: $E_{P_{li}}$ = annual wind power potential (MWh); ρ = air density (kg/m^3); A_r = area swept by the rotor (m^2); v = average wind speed (m/s); C_P = drag coefficient rotor power (adimensional); η = efficiency of the generator-set mechanical and electrical transmissions (adimensional).

Custodio [56] explains that for the conversion of wind energy, it is important to study the vertical behavior of the wind in the boundary layer of the surface, where wind turbines are usually located. The aforementioned author points out that in this aspect, the roughness length (z0) is the average height of the soil protrusions, responsible for the frictional force that opposes the movement of the air mass, resulting in a reduced wind velocity near the ground. Therefore, it can be deduced that, due to the influence of the viscosity of the air in contact with the terrain, it generates a wind profile whose velocity varies with height (h). To determine the wind speed at another time, it is possible to use the logarithmic wind speed behavior, as indicated by Eq. (16):

$$\frac{v_1}{v_2} = \frac{\ln\left(\frac{h_1}{z_0}\right)}{\ln\left(\frac{h_2}{z_0}\right)} \quad (16)$$

The formulation indicated in Eq. (16) was used, since the original average monthly wind speed data collected in the SWERA [57] database are for a height of 10 m. Data from the wind turbines of the manufacturer Enercon were also used, with power ratings equivalent to 2 MW, 3 MW, 3.5 MW, and 7.5 MW [58]. Thus, the wind velocity for wind turbine height was calculated from Eq. (16), which is: 135 m for wind turbines of 3 MW and 7.5 MW, 138 m for those of 2 MW, and 74 m for 3.5 MW. Similar to the study by Aquila et al. [43], a value of $\eta = 0.98$ was considered and the areas scanned for each type of wind turbine are shown in Table 4. The soil roughness coefficient data for each city are available in CEPEL [59] and the normal atmospheric density (ρ) = 1.225 kg/m^3 was considered for all calculations.

Table 4
Area swept by rotor in each type of aerogenerator.

Wind turbine power (MW)	Area swept by rotor (m^2)
2 MW	5281
3 MW	10,515.5
3.5 MW	8012
7.5 MW	12,668

It is important to note that, to calculate the potential of each wind energy plot, combinations of wind turbines were defined such that the highest possible wind energy production would be achieved in each of the nine scenarios. Table 5 lists the types and quantity of wind turbines for each installed wind power scenario.

Another important detail regarding the calculation of wind potential, observed by Custodio [56] and Aquila et al. [1], is that C_P varies according to wind speed. To adjust the C_P value according to each wind velocity collected, cubic regressions were performed in Minitab® software. Four cubic regression equations—one for each turbine size—were elaborated from wind turbine C_P data for 20 wind speeds (0–20 m/s) (see Appendix A).

The regression adjustments for the 2 MW, 3 MW, 3.5 MW, and 7.5 MW wind turbines reached a R^2_{adj} of 94.6%, 92.1%, 94.3%, and 91.4%, respectively, and are considered suitable based on Hair Jr. et al. [60]. The following regressions are presented for wind turbines of 2 MW (Eqs. (17)), 3 MW (Eqs. 18), 3.5 MW (Eqs. (19)), and 7.5 MW (Eq. (20)):

$$C_{P_{2MW}} = -0.09843 + 0.1796v - 0.01668v^2 + 0.000406v^3 \quad (17)$$

$$C_{P_{3MW}} = -0.01092 + 0.1813v - 0.01782v^2 + 0.000406v^3 \quad (18)$$

$$C_{P_{3.5MW}} = -0.09513 + 0.1643v - 0.01451v^2 + 0.000336v^3 \quad (19)$$

$$C_{P_{7.5MW}} = -0.01073 + 0.1562v - 0.0125v^2 + 0.000261v^3 \quad (20)$$

3.3.2. PV power production

For the calculation of the portion representing the average annual production of solar energy, the data of PV cells with the following characteristics were used [61]: nominal power of the cell (P_{nom}) = 300 W; efficiency (η) = 15.50%; area (A) = 1.94 m^2; temperature loss coefficient above 25 °C (σ_T) = −0.42%/°C. For the scenario with

Table 5
Combination of wind turbines for each wind power scenario.

Installed wind power	Combination of wind turbines
30 MW	10 wind turbines of 3 MW
24 MW	8 wind turbines of 3 MW
22.5 MW	5 wind turbines of 3 MW and 1 wind turbines of 7.5 MW
18 MW	6 wind turbines of 3 MW
15 MW	5 wind turbines of 3 MW
12 MW	4 wind turbines of 3 MW
7.5 MW	2 wind turbines of 2 MW and 1 wind turbines of 3.5 MW
6 MW	2 wind turbines of 3 MW
0 MW	None

100% solar power, the use of 100,000 PV cells was assumed, and for the other scenarios, cell quantity was assumed to be proportional to the percentage of solar power installed (% solar x 100,000).

Monthly solar irradiance data, according to latitude and mean temperature (T) for each city, were also collected from the SWERA [57] database. 25% losses were considered for the energy produced, which, according to ABINEE [62], occur due to: shading, accumulation of dust in the cells, losses in the inverters, losses due to unavailability, differences in the characteristic curves of the modules, and losses in cabling. The loss due to the increase of each degree of temperature above 25 °C (ambient temperature), calculated in a specific way according to the temperature of each city, was also discounted.

With the data described, it was possible to estimate the average annual production of solar energy for hybrid powerplants in each scenario and for each city. In Eq. (21), the calculation for the production of solar energy is shown.

$$E_{p_{FV}} = 0.8\eta I_m A(1 - \sigma_T T) \tag{21}$$

where: $E_{p_{FV}}$ = PV potential energy (MWh); η = efficiency (%); I_m = average irradiation in the period (kWh/m^2); A = area (m^2); σ_T = temperature loss coefficient (%/°C); T = temperature (°C).

As indicated in Eq. (22), it is now possible to obtain the average annual production of total energy by means of the sum of the calculated wind and PV energies, which corresponds to the PG of the wind-PV powerplant.

$$E_{P_{total}} = E_{P_e} + E_{p_{FV}} \tag{22}$$

where: $E_{P_{total}}$ = total energy production, corresponding to the PG (MWh).

4. Application and results

The application of the proposed method is divided into the following steps: calculation of the responses for each scenario indicated in the mixture arrangement, obtaining the objective functions, applying the NBI and choosing the optimal solution at the Pareto frontier, as shown in Fig. 2.

4.1. Formulation of objective functions from mixture arrangement

To determine the reduced emission density and LCOE for each scenario of the arrangement, the PG was initially calculated for each scenario illustrated in Appendix B. In the reduced emission density calculations, the formula described in Eq. (8) was applied, and the value for the adopted emission factor was 0.0817 tCO_2/MWh, equivalent to the last annual emission factor published by MCTIC [63] for the year 2016. This factor represents average CO_2 emissions for power generation in the context of the Brazilian market and considers all energy sources—including wind and PV [63]. Since wind and PV plants do not emit CO_2 during operation, their use contributes to a reduction of overall system emissions, based on the emission factor previously presented.

In calculating the LCOE values, a discount rate of 8.42%—calculated by the WACC—and the PG values shown in Appendix B were used. To obtain the investment value for both wind and solar power generation, based on data from CCEE [5], the average investment value per installed power for projects contracted since 2014 were calculated for each source. The average investment value for wind power was found to be R$ 3918,623.32 per installed MW, whereas that of solar was R$ 4795,304.68 per installed MW. As these are not real projects, the values of investment by city were not discriminated.

In relation to O&M costs, the value was calculated based on the investment value. The calculation basis was obtained from Mudasser et al. [64] and the study by Aquila et al. [1], and amounts to 2% of the total investment value for a wind farm. For a solar plant, O&M costs are equal to 0.5% of the total investment [62]. As for interest on financing, a value of 4.99%—as indicated in Section 3.1—was used in each scenario.

With the values of y_1 (reduced emission density) and y_2 (LCOE) calculated for all scenarios in each city and indicated in Appendix C, it was possible to estimate the objective functions. For this, quadratic regressions (Eqs. (23) and (24)) were performed by the Minitab ® software, and for y_1 it was necessary to include two additional terms for the model to have an ideal fit, based on Hair Jr. [60]. For y_2, it was not necessary to add the terms, and in Table 6 and 7 are described to Eqs. (25)–(48), with the objective functions for y_1 and y_2.

$$E(y) = \sum_{i=1}^{q} \beta_i x_i + \sum \sum_{i<j}^{q} \beta_{ij} x_i x_j \tag{23}$$

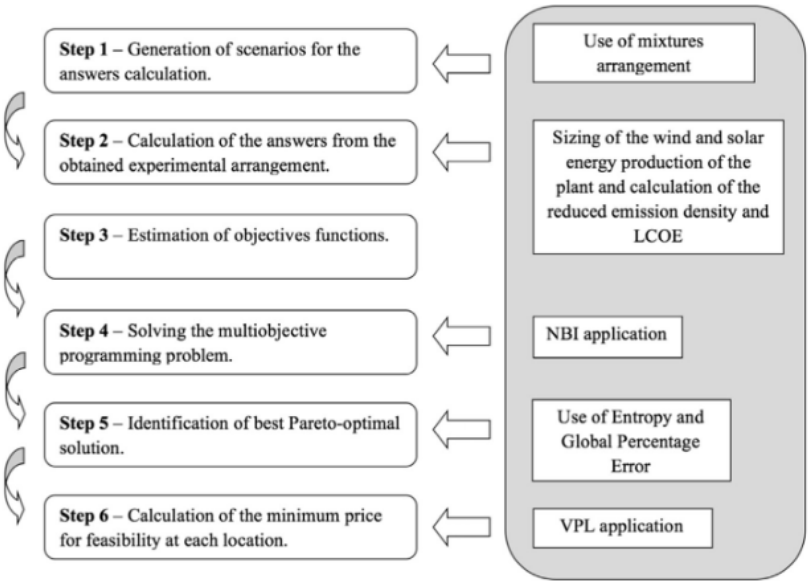

Fig. 2. Proposed method flowchart.

Table 6
Target function for reduced emission density (y_1) in each city.

Cities	R^2_{adj}	y_1	
Araripina-PE	99.34%	$3.83x_1 + 20.53x_2 - 29.49x_1x_2 + 33.98x_1x_2(x_1 - x_2) - 36.85x_1x_2(x_1 - x_2)^2$	(25)
Braganca Paulista-SP	99.65%	$1.79x_1 + 19.02x_2 - 30.32x_1x_2 + 34.73x_1x_2(x_1 - x_2) - 35.25x_1x_2(x_1 - x_2)^2$	(26)
Campo Grande-MS	99.51%	$2.64x_1 + 19.03x_2 - 29.01x_1x_2 + 33.85x_1x_2(x_1 - x_2) - 36.07x_1x_2(x1 - x_2)^2$	(27)
Jundiai-SP	99.48%	$2.49x_1 + 17.30x_2 - 26.12x_1x_2 + 30.10x_1x_2(x_1 - x_2) - 31.80x_1x_2(x_1 - x_2)^2$	(28)
Laguna-SC	99.38%	$2.74x_1 + 16.16x_2 - 23.71x_1x_2 + 27.32x_1x_2(x_1 - x_2) - 29.43x_1x_2(x_1 - x_2)^2$	(29)
Macau-RN	99.52%	$2.83x_1 + 20.45x_2 - 29.92x_1x_2 + 36.78x_1x_2(x_1 - x_2) - 38.45x_1x_2(x_1 - x_2)^2$	(30)
Mineiros-GO	99.33%	$3.52x_1 + 19.25x_2 - 27.79x_1x_2 + 32.06x_1x_2(x_1 - x_2) - 34.79x_1x_2(x_1 - x_2)^2$	(31)
Montes Claros-MG	99.47%	$3.13x_1 + 20.72x_2 - 31.05x_1x_2 + 35.80x_1x_2(x_1 - x_2) - 37.95x_1x_2(x_1 - x_2)^2$	(32)
Mossoro-RN	99.19%	$3.29x_1 + 20.70x_2 - 31.46x_1x_2 + 34.45x_1x_2(x_1 - x_2) - 36.02x_1x_2(x_1 - x_2)^2$	(33)
Parnaiba-PI	99.61%	$2.71x_1 + 21.70x_2 - 33.46x_1x_2 + 38.26x_1x_2(x_1 - x_2) - 38.26x_1x_2(x_1 - x_2)^2$	(34)
Rio Grande-RS	99.40%	$2.83x_1 + 16.48x_2 - 24.10x_1x_2 + 27.70x_1x_2(x_1 - x_2) - 29.97x_1x_2(x_1 - x_2)^2$	(35)
Xique-Xique-BA	99.42%	$3.50x_1 + 21.38x_2 - 31.46x_1x_2 + 36.42x_1x_2(x_1 - x_2) - 38.93x_1x_2(x_1 - x_2)^2$	(36)

Table 7
Objective function for LCOE (y_2) in each city.

Cities	R^2_{adj}	y_2	
Araripina-PE	96.19%	$141.93x_1 + 440.65x_2 - 220.35x_1x_2$	(37)
Braganca Paulista-SP	84.18%	$291.18x_1 + 445.57x_2 - 28.98x_1x_2$	(38)
Campo Grande-MS	93.06%	$197.55x_1 + 486.94x_2 - 158.61x_1x_2$	(39)
Jundiai-SP	93.66%	$211.03x_1 + 530.59x_2 - 207.48x_1x_2$	(40)
Laguna-SC	95.25%	$195.72x_1 + 563.15x_2 - 304.16x_1x_2$	(41)
Macau-RN	94.37%	$181.16x_1 + 455.14x_2 - 227.49x_1x_2$	(42)
Mineiros-GO	95.85%	$153.71x_1 + 470.83x_2 - 289.18x_1x_2$	(43)
Montes Claros-MG	94.30%	$168.95x_1 + 442.04x_2 - 191.37x_1x_2$	(44)
Mossoro-RN	92.05%	$164.83x_1 + 435.09x_2 - 172.51x_1x_2$	(45)
Parnaiba-PI	94.00%	$193.32x_1 + 422.68x_2 - 118.74x_1x_2$	(46)
Rio Grande-RS	95.53%	$190.13x_1 + 551.39x_2 - 306.32x_1x_2$	(47)
Xique-Xique-BA	95.12%	$152.02x_1 + 426.84x_2 - 217.51x_1x_2$	(48)

$$E(y) = \sum_{i=1}^{q} \beta_i x_i + \sum \sum_{i<j}^{q} \beta_{ij} x_i x_j + \sum \sum_{i<j}^{q} \beta_{ij(i-j)} x_i x_j \left(x_i - x_j \right) + \sum \sum_{i<j}^{q} \beta_{ij(i-j)^2} x_i x_j (x_i - x_j)^2 \quad (24)$$

It is observed that, for each city, objective functions with different coefficients were obtained for both y_1 and y_2. This reveals that it was possible to determine the objective functions modeled according to the wind and solar potential of each city.

4.2. Results of NBI optimization

After obtaining the objective functions for each city, the next step is the resolution of the multiobjective problem through the NBI. In this way, the payoff matrix is assembled, as indicated in Eq. (3). Subsequently, it is possible to solve the optimization problem with the NBI formulation presented in Eq. (2). It should be noted that restrictions on the mixing problem were added, which correspond to $x_1 + x_2 + ...+x_p = 1$ and $0 \leq x_p \leq 1$.

From the results of the NBI, the Pareto frontier was constructed equispaced and evenly distributed, with weights varying with an increase of 0.05. Finally, from the measure of the entropy and GPE ratio described in Eq. (6), it was possible to identify the optimal plant configuration for each city, as shown in Figs. 3, 4, and 5.

Most of the cities presented different percentages of wind and solar power in the optimal configuration, as well as different values for y_1 and y_2. Thus, it is possible to consider that the model responds adequately as a criterion in the bidding process for wind-PV contracts in Brazil.

It is important to highlight that, in relation to optimal configurations between cities, the most adequate solution is not always that which indicates the same importance for the objective functions. In Araripina-PE, for example, the optimal configuration is at a border point where the weight to maximize the reduced emission density is at 10%, while for the LCOE minimization, the weight is at 90%. In Jundiai-SP, the optimal solution is at the point where the weight to maximize the reduced emission density is at 15%, while for the LCOE minimization, the weight is at 85%. In Table 8, the results of maximizing y_1 and minimizing y_2 are simultaneously weighted for each objective function at the point with the Pareto-optimal solution, where w_1 is the weight for the reduced emission density function and w_2 is the weight for the LCOE function. Additionally described in the table is the ratio of y_1 / y_2 which makes it possible to rank cities where reduced emission density is maximized at a lower cost.

The ratio of y_1/y_2 shows that in Araripina-PE it is possible to avoid a large amount of CO_2 emission per area (tCO_2/km^2), with the lowest LCOE (R$/MWh). Put differently, it is where the greatest socio-environmental benefit is available at the lowest cost. The cities of Xique Xique-BA and Mineiros-GO show the best results, with all cities in the Northeast region having a higher ratio of y_1 / y_2 than cities in other regions of the country—except Mineiros-GO and Montes Claros-MG.

As observed, the PG value is necessary for the calculations of y_1 and y_2. Therefore, from the optimal results of y_1 and y_2, it is possible to extract the PG value from the plant in its optimal configuration, as shown in Table 8. In this way, it is possible to conclude that when considering objectives that depend on the PG value, the model also contributes to the determination of a PG that is compatible with the objective of maximizing the socioeconomic benefit of the electricity sector. The results of the PG reinforce the wind and solar potential of the northeast region (for example, the cities of Araripina-PE, Xique-Xique-BA, Mossoro-RN, and Macau-RN). Additionally, the cities of Mineiros-GO and Montes Claros-MG can also be seen as potential locations for wind-PV plants.

The results of the cities of Mineiros-GO and Montes Claros-MG can be considered as surprising, since they are located in regions that do not yet have wind and PV power generation projects. The city of Mineiros-GO presented the second highest level of reduced emission density and the third lowest LCOE—superior to several cities in the northeast region where the majority of wind and solar projects are installed, and surpassing Rio Grande-RS, located in a state that has already installed wind powerplants.

Montes Claros-MG, located in the north of Minas Gerais, presented

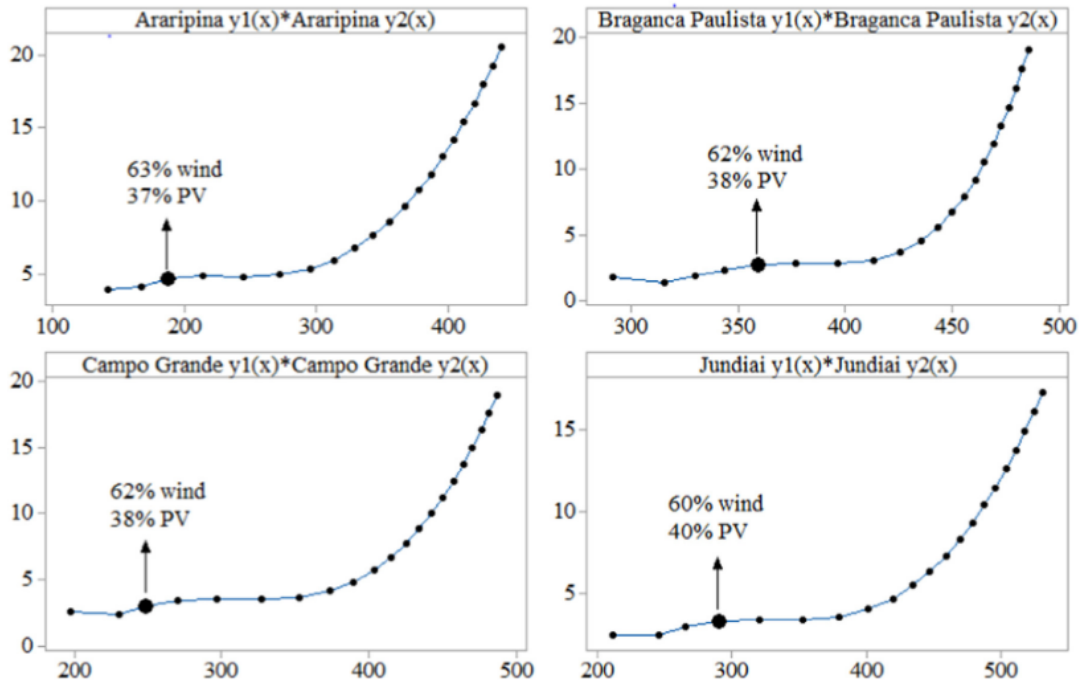

Fig. 3. Pareto frontier and optimal configuration in Araripina, Braganca Paulista, Campo Grande, and Jundiai.

results for reduced emission density and LCOE superior to those of the city of Parnaiba-PI—already hosting wind power projects. This result reveals Brazil's potential for the use of wind and solar energy in regions not yet exploited and the importance for wind-PV power projects to take advantage of this potential in a rational way. In Jundiai and Braganca Paulista, the least-favorable results were observed. However, if the weight of the objective functions is changed, the results for these cities improve, as seen in Fig. 6.

Similarly, Fig. 6 illustrates that the choice of which project should be contracted is subject to change. For example, if the emission density was greater than 50%, the city of Laguna-SC—rather than Braganca Paulista-SP—would become the least-favorable option for plant installation. The same occurs with the order of the best place for the installation of the project. When a weight upwards of 65% is applied for the emission density function, it is observed that Xique-Xique-BA becomes the most-favorable location to install the plant, with Araripina-

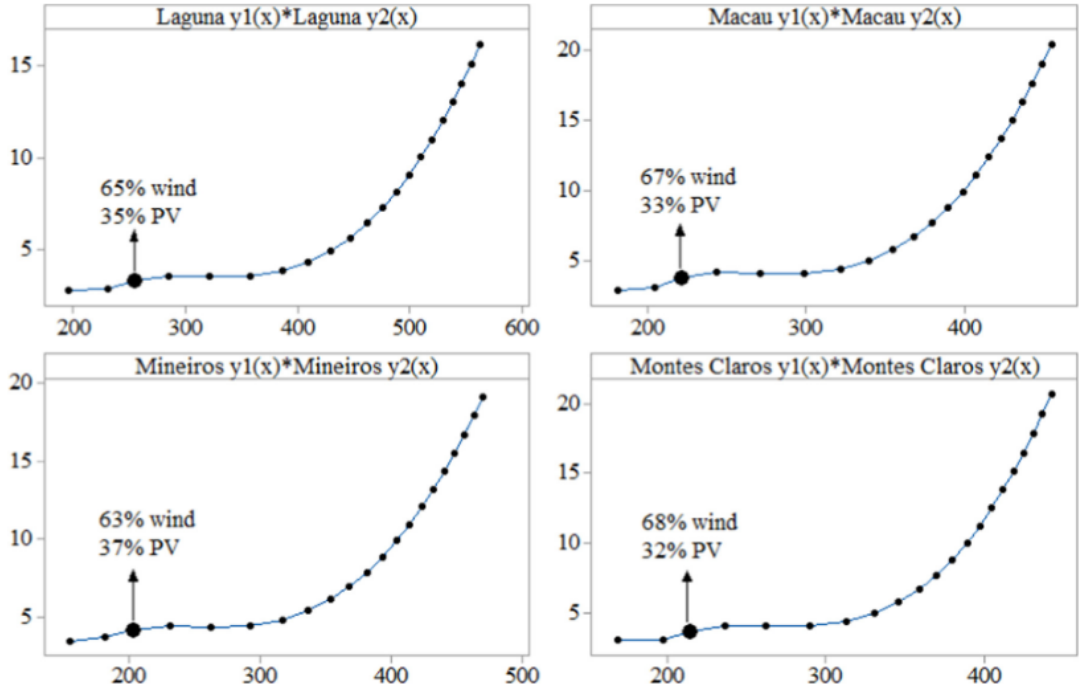

Fig. 4. Pareto frontier and optimal configuration in Laguna, Macao, Mineiros, and Montes Claros.

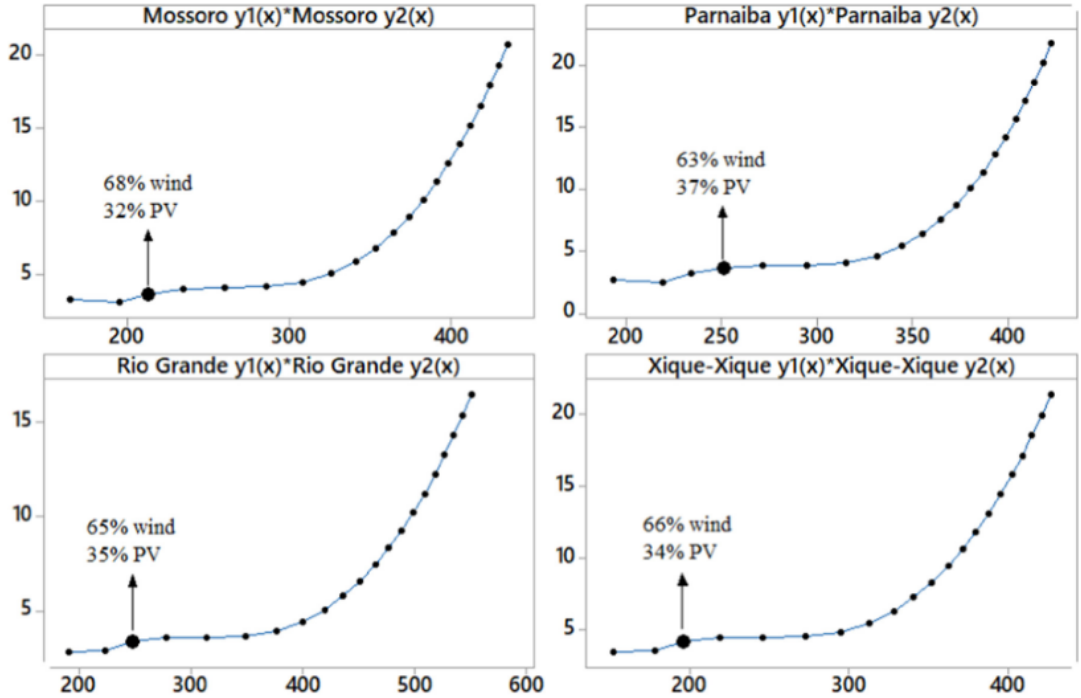

Fig. 5. Pareto frontier and optimal configuration in Mossoro, Parnaiba, Rio Grande, and Xique-Xique.

Table 8
Weight of the objective functions at the optimum configuration point of the plant.

Cities	w_1	w_2	y_1	y_2	y_1/y_2	PG
Araripina-PE	10%	90%	4.62	187.58	0.0246	109500.90
Xique-Xique-BA	10%	90%	4.21	196.16	0.0215	104660.81
Mineiros-GO	10%	90%	4.25	202.60	0.0210	101527.38
Montes Claros-MG	10%	90%	3.72	214.30	0.0174	95103.39
Mossoro-RN	10%	90%	3.68	212.92	0.0173	94272.73
Macau-RN	10%	90%	3.79	221.02	0.0171	95233.12
Parnaiba-PI	15%	85%	3.64	250.86	0.0145	86303.03
Rio Grande-RS	10%	90%	3.41	247.17	0.0138	83182.01
Laguna-SC	10%	90%	3.29	254.09	0.0129	80917.27
Campo Grande-MS	15%	85%	3.45	269.96	0.0128	81030.29
Jundiai-SP	15%	85%	3.29	289.70	0.0114	74653.88
Braganca Paulista-SP	20%	80%	2.69	358.82	0.0075	62800.70

PE falling behind Parnaiba-PI.

This indicates that the optimal configuration selection method should be clear and defined to avoid uncertainties for investors when choosing the best location for a wind-PV powerplant. The proposed method for selecting the optimum configuration sought, through entropy, to take into account the country's goal of seeking to diversify the energy matrix and the GPE to evaluate the distance of optimal solutions to the utopia line, that is, a related question to the applied optimization method.

However, for practical applications, decision makers can determine other criteria that can be either quantitative or subjective. If the government needs to emphasize socio-environmental aspects, a criterion can be adopted to prioritize this objective. The same can be done toward prioritizing the reduction of the LCOE.

Another aspect to be highlighted is the importance of the NBI in applying a method to determine the optimal configuration. The NBI allows the construction of the Pareto frontier in an equispaced way—independent of the increment used for the weights of the functions. The use of another method could present faults in the frontier construction and hamper the process of selecting the optimal configuration.

Fig. 7 reveals some curiosities between the wind and PV potentials of cities that are in close proximity. Jundiai-SP and Braganca Paulista-SP, for example, are almost neighboring cities. However, it can be seen in Fig. 7 that in the configuration of the project with 100% wind power, Jundiai-SP demonstrates a wind potential far superior to that of Braganca Paulista-SP. Conversely, when the project with 100% PV power is analyzed, Braganca Paulista-SP surpasses Jundiai-SP, revealing a superior PV potential.

It can be considered that the proposed method was able to contribute to decision-making in the selection of wind-PV projects. From the model, it was possible to find the optimum configuration (percentage) of wind and PV power generation, as well as the responses to low emission density and LCOE, taking into account the specific wind and PV potential of each site. It is worth mentioning that each tool used in the construction of the method was determinant of the results and can be applied in practical situations.

Finally, it is important to highlight that the model proposed in this study may be useful for regulators in the Brazilian electricity sector to determine the potential entrepreneurs of wind-PV hybrid farms to configure their projects in a way that maximizes the socioeconomic and environmental benefits provided by the two sources. By constructing a method that requires the producer to set up the wind-PV farm in a way that optimizes the benefits to society, potential investors will subsequently be able to compete in lower-priced auctions for alternative energy sources in the country.

5. Conclusions

This study used multiobjective programming from the NBI to present a contribution to guide the contracting of wind-PV power generation projects in Brazil. Multiobjective programming allows for the simultaneous optimization of functions related to the reduced emission density and LCOE in the proposed model, thus optimizing the environmental and socioeconomic gains, respectively.

Based on the constructed model, it is possible for the government to

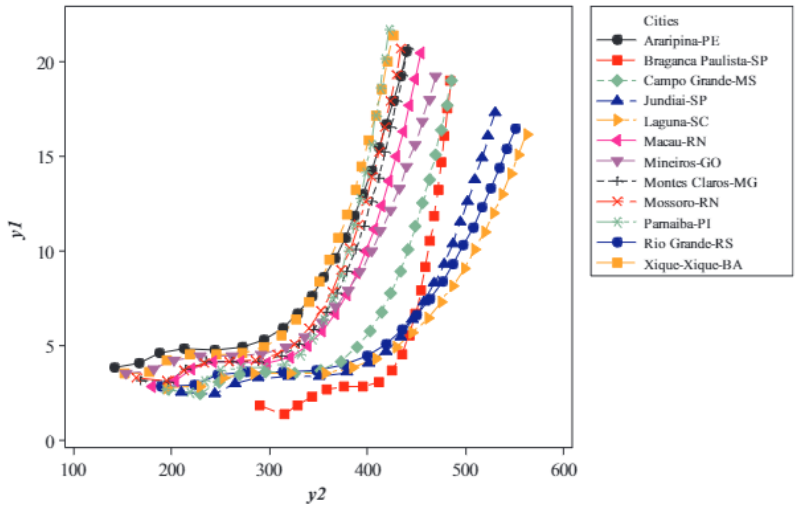

Fig. 6. Pareto frontiers of all analyzed cities.

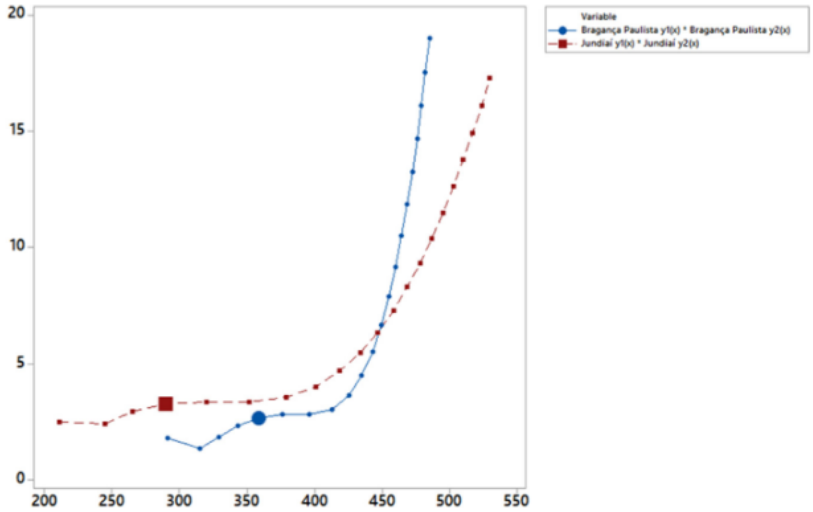

Fig. 7. Pareto frontiers for Braganca Paulista-SP and Jundiai-SP.

determine that the wind-PV projects participating in lower-priced auctions are optimally configured to meet the objective of maximizing the socioeconomic well-being produced by the electricity sector.

Additionally, a method for decision making based on the ratio between entropy (which meets the objectives of diversifying the Brazilian energy matrix) and GPE (which allows us to find the solution closest to utopia) was used to determine the Pareto-optimal solution.

It can be considered that the gains provided by the construction of wind-PV plants are distributed in an equitable way with the application of the model. This is because, with the simultaneous optimization of the functions considered in the study, both the environmental preservation of the place where the plant is built seeks to be preserved, and the cost to the energy producer is to be reduced. In addition, the legislators and final consumers will benefit, because once the optimal configuration is determined from the proposed model, the projects will be able to compete in lower-priced auctions, and the less-costly project in its optimal configuration will be contracted.

It is worth mentioning that the steps of the present model can be replicated to configure any on-grid wind-PV plant which is part of an electric system that is based on the physical guarantee quota regime.

The results indicate the efficiency of the model as it was possible to identify optimal levels of inputs and outputs compatible with the specific characteristics of wind potential and PV for twelve different cities. It was also possible to verify that in some cities located in regions of Brazil where there are still no wind and PV plants installed, there is good potential for the use of wind-PV power generation. Additionally, in Brazil, even between cities of close proximity, there are different wind and PV profiles, which indicates that the location of the project is fundamental for the best use of each source.

Finally, it is important to point out that the proposed model is a first contribution to help in the contracting of wind-PV power generation projects in Brazil. Future work is of great value in order to develop new models or to improve the model proposed in this work.

Acknowledgments

The authors would like to thank the Brazilian Government agencies CNPq, CAPES, and FAPEMIG for their support.

Appendix A

see Table A1

Table A1
Data used for C_p regression x wind speed.

v	v^3	C_p (2 MW)	C_p (3 MW)	C_p (3.5 MW)	C_p (7.5 MW)
0	0	0.00	0.00	0.00	0.00
1	1	0.00	0.00	0.00	0.00
2	8	0.12	0.058	0.08	0.00
3	27	0.29	0.279	0.28	0.263
4	64	0.40	0.376	0.37	0.352
5	125	0.43	0.421	0.41	0.423
6	216	0.46	0.451	0.44	0.453
7	343	0.48	0.469	0.46	0.470
8	512	0.49	0.470	0.47	0.478
9	729	0.50	0.445	0.47	0.477
10	1000	0.49	0.401	0.46	0.483
11	1331	0.42	0.338	0.43	0.470
12	1728	0.35	0.270	0.38	0.429
13	2197	0.29	0.212	0.32	0.381
14	2744	0.23	0.170	0.26	0.329
15	3375	0.19	0.138	0.21	0.281
16	4096	0.15	0.114	0.17	0.236
17	4913	0.13	0.095	0.15	0.199
18	5832	0.11	0.080	0.12	0.168
19	6859	0.09	0.068	0.10	0.142
20	8000	0.08	0.058	0.09	0.122

Appendix B

see Table B1

Table B1
Physical guarantee (MWh) for each scenario in each city.

	100% wind power	80% wind power 20% PV	75% wind power 25% PV	60% wind power 40% PV	50% wind power 50% PV	40% wind power 60% PV	25% wind power 75% PV	20% wind power 80% PV	100% PV
Araripina-PE	137,560	119,555	99,359	101,549	92,546	83,544	60,020	65,539	47,533
Braganca Paulista-SP	63,551	59,654	50,616	55,757	53,808	51,860	43,304	47,962	44,065
Campo Grande - MS	94,159	83,754	69,862	73,409	69,121	63,034	47,637	52,659	44,083
Jundiai-SP	89,211	79,382	65,996	69,552	64,637	59,722	44,785	49,882	40,062
Laguna-SC	98,191	86,040	71,050	73,889	67,814	61,738	44,885	49,887	37,436
Macau-RN	101,286	90,500	90,378	79,713	86,694	68,927	53,488	58,141	47,355
Mineiros-GO	126,458	110,083	91,225	93,708	85,520	77,332	55,397	60,957	44,581
Montes Claros-MG	111,894	99,114	82,503	86,333	79,943	73,552	54,967	60,772	47,992
Mossoro-RN	117,807	103,835	77,638	89,863	74,610	75,892	57,000	61,920	47,948
Parnaiba-PI	96,645	87,373	73,982	78,102	73,467	68,831	55,006	59,561	50,290
Rio Grande-RS	101,547	88,510	73,387	76,196	69,858	63,520	46,296	50,844	38,169
Xique-Xique-BA	125,528	110,323	91,860	95,120	87,518	79,916	58,427	64,712	49,508

Appendix C

see Tables C1 and C2

Table C1
Values of y_1 (tCO_2/km^2) for each scenario and in each city.

	100% wind power	80% wind power 20% PV	75% wind power 25% PV	60% wind power 40% PV	50% wind power 50% PV	40% wind power 60% PV	25% wind power 75% PV	20% wind power 80% PV	100% PV
Araripina-PE	3.784	4.047	3.569	4.467	4.787	5.245	5.546	7.185	20.547
Braganca Paulista-SP	1.748	2.019	1.818	2.452	2.783	3.256	4.001	5.258	19.048
Campo Grande - MS	2.590	2.836	2.503	3.229	3.575	3.957	4.401	5.773	19.956
Jundiai-SP	2.454	2.687	2.370	3.059	3.343	3.750	4.138	5.470	17.318
Laguna-SC	2.701	2.912	2.552	3.250	3.508	3.876	4.147	5.436	16.183
Macau-RN	2.786	3.063	3.246	3.506	4.484	4.327	4.942	6.374	20.471
Mineiros-GO	3.479	3.726	3.276	4.124	4.424	4.855	5.118	6.683	19.271
Montes Claros-MG	3.078	3.355	2.963	3.797	4.135	4.618	5.054	6.663	20.746
Mossoro-RN	3.240	3.515	2.788	3.952	3.859	4.764	5.266	6.786	20.727
Parnaiba-PI	2.659	2.957	2.657	3.435	3.800	4.321	5.082	6.530	21.739
Rio Grande-RS	2.793	2.996	2.636	3.351	3.613	3.988	4.278	5.574	16.499
Xique-Xique-BA	3.453	3.734	3.300	4.184	4.527	5.017	5.398	7.095	21.401

Table C2
Values of y_2 (R$/MWh) for each scenario and in each city.

	100% wind power	80% wind power 20% PV	75% wind power 25% PV	60% wind power 40% PV	50% wind power 50% PV	40% wind power 60% PV	25% wind power 75% PV	20% wind power 80% PV	100% PV
Araripina-PE	131.97	156.93	190.36	190.74	212.58	239.13	340.44	314.09	445.85
Braganca Paulista-SP	285.67	314.52	373.68	347.40	365.63	385.22	471.86	429.19	480.94
Campo Grande - MS	192.81	223.93	271.43	263.86	284.63	316.93	428.94	390.91	480.75
Jundiai-SP	203.50	236.35	286.59	278.50	304.37	334.51	456.25	412.59	529.00
Laguna-SC	184.89	218.06	266.21	262.15	290.11	323.59	455.24	415.13	566.11
Macau-RN	179.24	207.32	209.28	242.99	226.93	289.83	382.01	354.05	447.53
Mineiros-GO	143.56	170.44	207.33	206.70	230.05	258.33	368.85	337.70	475.38
Montes Claros-MG	162.25	189.30	229.25	224.36	246.10	271.61	373.57	338.73	441.59
Mossoro-RN	154.10	180.69	243.62	215.55	263.69	263.24	358.48	332.45	442.00
Parnaiba-PI	187.85	214.74	255.66	248.01	267.79	290.24	371.47	345.62	421.42
Rio Grande-RS	178.78	211.98	257.73	254.21	281.62	314.51	441.36	404.87	555.25
Xique-Xique-BA	144.63	170.07	205.90	203.64	224.80	249.98	349.72	318.11	428.07

References

[1] Aquila G, Rocha LCS, Rotela Junior P, Pamplona EO, Queiroz AR, Paiva AP. Wind power generation: an impact analysis of incentive strategies for cleaner energy provision in Brazil. J Clean Prod 2016;137:1100–8.

[2] Pereira Jr. AOP, Pereira AS, La Rovere EL, Barata MML, Villar SC, Pires SH. Strategies to promote renewable energy in Brazil. Renew Sustain Energy Rev 2011;15. [681-68].

[3] Aquila G, Pamplona EO, Queiroz AR, Rotela P, Fonseca MN. An overview of incentive policies for the expansion of renewable energy generation in electricity power systems and the Brazilian experience. Renew Sust Energ Rev 2017;70:1090–8.

[4] Schmidt J, Cancella R, Pereira Jr. A. An optimal mix of solar PV, wind and hydro power for a low-carbon electricity supply in Brazil. Renew Energy 2016;85:137–47.

[5] CCEE. - Câmara de Comercialização de Energia Elétrica. O que fazemos: Leilões; 2017. Available at: ⟨http://www.ccee.org.br/portal/faces/oquefazemos_menu_lateral/leiloes?_afrLoop=5547777042548#%40%3F_afrLoop%3D5547777042548%26_adf.ctrl-stat%3Dp6tr9dqjl_112⟩. [Accessed july 2017].

[6] EPE – Empresa de Pesquisa Energética. Avaliação da geração de usinas híbridas eólico-fotovoltaicas: Proposta metodológica e estudos de caso, EPE, Rio de Janeiro; 2017. p. 32.

[7] Trannin M. Desafios e oportunidades para a geração de energia elétrica por fontes renováveis no Brasil: Estudo de caso sobre a Usina de Tacaratu (PE). FGV Energia; 2016.

[8] Fadigas EAFA. Energia eólica. Manole: Barueri; 2011. p. 285.

[9] Ramanathan R. Comparative risk assessment of energy supply technologies: a data envelopment analysis approach. Energy 2001;26:197–203.

[10] Van der Zwann B, Rabl A. Propescts for PV: a learning curve analysis. Sol Energy 2003;74:19–31.

[11] REN 21. Global status report; 2016. Available at: ⟨http://www.ren21.net/wp-content/uploads/2016/06/GSR_2016_Full_Report.pdf⟩. [Accessed july 2017].

[12] Ramli MAM, Hiendro A, Al-Turki YA. Techno-economic energy analysis of wind/solar hybrid system: case study for western coastal area of Saudi Arabia. Renew Energy 2016;91:374–85.

[13] Kaabeche A, Belhamel M, Ibtiouen R. Sizing optimization of grid-independent hybrid photovoltaic/wind Power generation system. Energy 2011;36:1214–22.

[14] Oree V, Hassen SZS, Fleming PJ. Generation expansion planning optimisation with renewable energy integration: a review. Renew Sustain Energy Rev 2017;69:790–803.

[15] Miettinen K. Nonlinear multiobjective optimization. Boston: Kluwer Academic Publishers; 1999.

[16] Baril C, Yacout S, Clément B. Design for six sigma through collaborative multi-objective optimization. Comput Ind Eng 2011;60(1):43–55.

[17] Shahraki AF, Noorossana R. Reliability-based robust design optimization: a general methodology using genetic algorithm. Comput Ind Eng 2014;74:199–207.

[18] Aghaei J, Amjady N, Shayanfar HA. Multi-objective electricity market clearing considering dynamic security by lexicographic optimization and augmented epsilon constraint method. Appl Soft Comput 2011;11:3846–58.

[19] Paiva AP, Ferreira JR, Balestrassi PP. A multivariate hybrid approach applied to AISI 52100 hardened steel turning optimization. J Mater Process Technol 2007;1–3(189):26–35.

[20] Charnes A, Cooper WW. Management models and industrial applications of linear progmmming. New York: John Wiley & Sons, Inc; 1961.

[21] Zhang W, Yang H. A study of the weighting method for a certain type of multi-criteria optimization problem. Comput Struct 2001;31(79):2741–9.
[22] Das I, Dennis JE. Normal boundary intersection: a new method for generating the Pareto surface in nonlinear multicriteria optimization problems. SIAM J Optim 1998;8(3):631–57.
[23] Park JB, Park YM, Won JR, Lee KY. An improved genetic algorithm for generation expansion planning. IEEE Trans Power Syst 2000;15:916–22.
[24] Kannan S, Slochanal SMR, Padhy NP. Application and comparison of metaheuristic techniques to generation expansion planning problem. IEEE Trans Power Syst 2005;20:466–75.
[25] Sirikum J, Techanitisawad A, Kachitivichyanukul V. New efficient GA-Benders' decomposition method: for power generation expansion planning with emission controls. IEEE Trans Power Syst 2007;22:1092–100.
[26] Aghaei J, Akbari MA, Roosta A, Gitizadeh M, Niknam T. Integrated renewable–conventional generation expansion planning using multiobjective framework. IET Gener Transm Distrib 2012;6:773–84.
[27] Meza JLC, Yildirim MB, Masud ASM. A model for the multiperiod multiobjective power generation expansion problem. IEEE Trans Power Syst 2007;22:871–8.
[28] Antunes CH, Martins AG, Brito IS. A multiple objective mixed integer linear programming model for power generation expansion planning. Energy 2004;29:613–27.
[29] Aghaei J, Akbari MA, Roosta A, Baharvandi A. Multiobjective generation expansion planning considering power system adequacy. Electr Power Syst Res 2013;102:8–19.
[30] Vahidinasab V, Jadid S. Normal boundary intersection method for suppliers' strategic bidding in electricity markets: an environmental/economic approach. Energy Convers Manag 2010;6(51):1111–9.
[31] Izadbakhsh M, Gandomkar M, Rezvani A, Ahmadi A. Short-term resource scheduling of a renewable energy based micro grid. Renew Energy 2015;75:598–606.
[32] Shannon CE. A mathematical theory of communication. Bell Syst Tech J 1948;27:379–423. [and 623–656, July and October].
[33] Rocha LCS, Paiva AP, Paiva EJ, Balestrassi PP. Comparing DEA and principal component analysis in the multiobjective optimization of P-GMAW process. J Braz Soc Mech Sci 2016;38(8):2513–26. https://doi.org/10.1007/s40430-015-0355-z.
[34] Rocha LCS, Paiva AP, Rotela Junior P, Balestrassi PP, Campos PH. Robust multiple criteria decision making applied to optimization of AISI H13 hardened steel turning with PCBN wiper tool. Int J Adv Manuf Technol 2017;89(5–8):2251–68.
[35] Bertoldi P, Rezessy S, Oikomonou V. Rewarding energy savings rather than energy efficiency: exploring the concept of a feed-in tariff for energy savings. Energy Policy 2013;56:526–35.
[36] Weida S, Kumar S, Madlener R. Financial viability of grid-connected solar PV and wind power systems in Germany. Energy Procedia 2016;106:35–45.
[37] Amarante OAC, Schultz DJ. Wind energy resource map of the state of Paraná, Brazil. Dewi Magazin, 15. 1999. p. 70–5.
[38] Shukla AK, Sudhakar K, Baredar P. Simulation and performance analysis of 110 kWp grid-connected photovoltaic system for residential building in India: a comparative analysis of various PV technology. Energy Rep 2016;2:82–8.
[39] ANEEL – Agência Nacional de Energia Elétrica. Atlas de energia elétrica do Brasil. 3ªed. Brasilia: ANEEL; 2008. p. 236.
[40] Branker K, Pathak MJM, Pearce JM. A review of solar photovoltaic levelized cost of electricity. Renew Energy Sustain Rev 2011;15:4470–82.
[41] Faria E, Barroso LA, Kelman R, Granville S, Pereira MV. Allocation of firm-energy rights among hydro plants: an Aumann-Shapley approach. IEEE Trans Power Syst 2009;24(2):541–51.
[42] Rocha LCS, Aquila G, Rotela Junior P, Paiva AP, Pamplona EO, Balestrassi PP. A stochastic economic viability analysis of residential wind power generation in Brazil. Renew Sust Energ Rev 2018;90:412–9.
[43] Aquila G, Rotela JR,P, Pamplona EO, Queiroz AR. Wind power feasibility analysis under uncertainty in the Brazilian electricity market. Energy Economics 2017;65:127–36.
[44] Ondraczek J, Komendantova N, Patt A. WACC the dog: the effect of financing costs on the levelized cost of solar PV power. Renew Energy 2015;75:888–98.
[45] Ertürk M. The evaluation of feed in tariff regulation of Turkey for onshore wind energy based on the economic analysis. Energy Policy 2012;45:359–67.
[46] UNFCCC – United Framework Convention on Climate Change. Guidelines on the assessment of investment analysis; 2012.
[47] ANEEL – Agência Nacional de Energia Elétrica, 2016. Nota Técnica no 33 /2016–SGT/ANEEL. Available at: 〈http://www2.aneel.gov.br/aplicacoes/audiencia/arquivo/2016/005/documento/ntecnica_33_sgt_ap_caiua.pdf〉. [Accessed july 2017].
[48] Damodaran A. Betas by sector (US); 2017. Available at: 〈http://people.stern.nyu.edu/adamodar/New_Home_Page/datafile/Betas.html〉. [Accessed july 2017].
[49] Sharpe W. Capital asset prices: a theory of market equilibrium under conditions of risk. J Financ 1964;19(3):425–42.
[50] Cornell J. Experiments with mixtures: designs, models, and the analysis of mixture data. 3rd ed. New York: John Wiley & Sons; 2002. p. 649.
[51] Montgomery DC. Design and analysis of experiments. 7th ed. New York: John Wiley & Sons; 2009. p. 665.
[52] Moreno R, Barroso LA, Rudnick H, Mocarquer S, Bezerra B. Auction approaches of long-term contracts to ensure generation investment in electricity markets: lessons from the Brazilian and Chilean experiences. Energy Policy 2010;38:5758–69.
[53] Amarante OAC. Atlas eólico. Minas Gerais. Belo Horizonte: CEMIG; 2010.
[54] COELBA - Companhia de Eletricidade do Estado da Bahia. Atlas do Potencial Eólico do Estado da Bahia; 2013.
[55] COPEL - Companhia Paranaense de Energia. Manual de avaliação técnico-econômica de empreendimentos eólio-elétricos. Curitiba: LACTEC; 2007. p. 104.
[56] Custódio RS. Energia eólica para a produção de energia elétrica. 2ed. Rio de Janeiro: Synergia; 2013.
[57] SWERA – Solar and Wind Energy Resource Assesment. National Renewable Energy Laboratory (NREL) maps; 2017. Available at: 〈https://maps.nrel.gov/swera/#/?aL=0&bL=groad&cE=0&lR=0&mC=40.21244%2C-91.625976&zL=4〉. [Accessed july 2017].
[58] ENERCON. Linha de produtos Enercon; 2015. Available at: 〈http://www.wobben.com.br/fileadmin/user_upload/ec_product_br.pdf〉. [Accessed july 2017].
[59] CEPEL – Centro de Pesquisas de Energia Elétrica. Atlas do Potencial Eólico Brasileiro; 2001. Available at: 〈http://www.cresesb.cepel.br/publicacoes/index.php?Task=livro&cid=1〉. [Accessed july 2017].
[60] Hair Jr. JF, Black WC, Babin BJ, Anderson RE. Multivariate Data Analysis. 7th ed. London: Pearson; 2014.
[61] Solar Yingli. Série de células YGE72; 2015. Available at: 〈http://www.yinglisolar.com/br/products/multicrystalline/yge-72-cell-series/〉. [Accessed in july 2017].
[62] ABINEE. Propostas para Inserção da Energia Solar Fotovoltaica na Matriz Brasileira. Brasília: ABINEE; 2012.
[63] MCTIC. - Ministério da Ciência, Tecnologia, Inovações e Comunicações. Arquivo dos fatores médios de emissão de CO2 grid mês/ano; 2017. Available at: 〈http://www.mctic.gov.br/mctic/opencms/textogeral/emissao_corporativos.html〉. [Accessed july 2017].
[64] Mudasser M, Yiridoe EY, Corscadden K. Economic feasibility of large community feed-in tariff-eligible wind energy production in Nova Scotia. Energy Policy 2013;62:966–77.